Steel and Composite Structures, *Vol. 30, No. 1* (*2019*) *1-12*
DOI: https://doi.org/10.12989/scs.2019.30.1.001

Equivalent reinforcement isotropic model for fracture investigation of orthotropic materials

Mahdi Fakoor*, Roham Rafiee and Shahab Zare

Faculty of New Sciences & Technologies, *University of Tehran*, *Tehran*, *Iran*

(*Received January 14, 2018, Revised December 29, 2018, Accepted December 31, 2018*)

Abstract. In this research, an efficient mixed mode I/II fracture criterion is developed for fracture investigation of orthotropic materials wherein crack is placed along the fibers. This criterion is developed based on extension of well-known Maximum Tensile Stress (MTS) criterion in conjunction with a novel material model titled as Equivalent Reinforced Isotropic Model (ERIM). In this model, orthotropic material is replaced with an isotropic matrix reinforced with fibers. A comparison between available experimental observations and theoretical estimation implies on capability of developed criterion for predicting both crack propagation direction and fracture instance, wherein the achieved fracture limit curves are also compatible with fracture mechanism of orthotic materials. It is also shown that unlike isotropic materials, fracture toughness of orthotic materials in mode I ($\boldsymbol{K_{Ic}}$|) cannot be introduced as the maximum load bearing capacity and thus new fracture mechanics property, named here as maximum orthotropic fracture toughness in mode I ($\boldsymbol{K_{Ic}}|^{\boldsymbol{ortho}}_{\boldsymbol{max}}$) is defined. Optimum angle between crack and fiber direction for maximum load bearing in orthotropic materials is also defined.

Keywords: orthotropic materials; fracture criterion; mixed mode; reinforced isotropic material; maximum tangential stress criterion

1. Introduction

Composite materials are widely used in various industries because of their unique properties and high strength to weight ratios (Deretic-Stojanovic and Kostic 2017, Serier *et al*. 2016). Composites show quasi-brittle behavior and the occurrence of fracture is unavoidable in them because of several induced cracks during manufacturing process (Merzoug *et al*. 2017). Thus, it is necessary to estimate damage and predict fracture in composites utilizing fracture mechanics theories to prevent catastrophic failure (Al-Fasih *et al*. 2018). In other words, developing fracture mechanics theories in composite materials play a significant role in design and analysis of composite materials for their engineering applications (Cetisli and Kaman 2014). Stress intensity factors and fracture toughness are the most important parameters in fracture mechanics of composites (Golewski 2017a, Sadowski and Golewski 2018, Faal *et al*. 2015). Sih *et al*. (1965) have obtained elastic stress distribution around crack tip and tried to consider stress intensity factor for anisotropic materials as a material parameter. Fracture toughness describes the resistance of a material against the propagation of cracks induced by experienced loadings (Golewski 2017b). Existence of notch or crack initiation and propagation accounts for accelerating the occurrence of fracture in orthotropic materials. Since most of the structures experience mixed mode in-plane loadings of mode I/II during their missions, developing a proper fracture criterion for predicting their fracture instance and load bearing capacity is of great importance (Fakoor and Khansari 2016, Lazzarin *et al*. 2014). In addition, fracture of composite materials in mode III loading is investigated in several references (Golewski 2017b, Aliha *et al*. 2015, Ehart *et al*. 1998). Wu (1967) presented a fracture criterion based on experimental observations on Balsa wood and glass fiber reinforced composites. One of the main shortcomings of this study can be found in practical problems for determining empirical constants. Hunt and Croager (1982) tried to obtain fracture toughness for pure mode II loadings utilizing results of finite element (FE) analysis, since no direct comparison was available between pure mode II in isotropic and orthotropic materials. They also developed a new criterion in terms of stress intensity factors for mixed mode I/II loading by curve fitting through experimental data on Baltic Red wood in presence of the cracks placed in RL plane. Mall *et al*. (1983) studied mixed mode fracture on eastern red spruce wood specimens in presence of center and edge cracks. Considering different direction for cracks and studying TL cracks, they found out that mode I and mode II can be correlated using fracture toughness. In their study, it was intended to investigate mixed mode on wood specimens and also presenting a proper fracture criterion based on experimental data. Chow and Woo (1979) concluded that a similar relationship presented by Wu can be applied to other types of wood. This relationship is very similar to maximum tensile stress employed for isotropic materials. Jernkvist (2001a)

*Corresponding author, Ph.D., Associate Professor,
E-mail: mfakoor@ut.ac.ir

http://www.techno-press.org/?journal=scs&subpage=6 ISSN: 1229-9367 (Print), 1598-6233 (Online)

introduced a mixed mode fracture criterion for induced cracks in longitudinal and transverse directions of composites by extending frequently used failure criteria of isotropic materials to orthotropic ones. His criterion was developed based on LEFM concepts and validated utilizing experimental observations on Norway spruce wood. He concluded that presented energy criteria for homogenous materials cannot be applied to orthotropic materials. He also extended Maximum Principal Stress (MPS) criterion for orthotropic materials. His analysis on both longitudinal and transverse cracks showed that MPS mixed mode criterion can be applied to both crack types (Jernkvist 2001b). He concluded that cracks always propagate along wood fiber direction. However his presented criterion is not valid for the specific region where $\frac{K_{II}}{K_I} > 3$ and this can be considered as a drawback in Jernkvist's presented model. As another shortcoming, this criterion neglects dissipated energy at the tip of the crack arisen from accumulation of micro-cracks. Moreover, due to linear nature of analysis, it can be considered as a conservative criterion and does not fit to experimental data appropriately. Van der Put (2007) presented a novel criterion using orthotropic-isotropic transformation. He has presented a similar form of Wu's criterion for elliptical flat cracks. He obtained real fracture energy and established a correlation between stress intensity factors and energy reduction rate. Non-local stress has been considered for fracture investigation of laminated composite materials (Li *et al*. 2012). Also, Romanowicz and Seweryn (2008) presented a fracture criterion for orthotropic materials relying on Non-local stress distribution. This criterion was developed for different crack orientation with respect to fiber direction and constructed based on growing micro-cracks in an elastic solid material. Presented criterion is in need of a damage factor which has not been characterized properly. This criterion has been extensively criticized in Anaraki and Fakoor (2010a). Anaraki and Fakoor (2010b) proposed a fracture criterion for orthotropic materials like wood subjected to mixed mode I / II loading. This criterion takes into account the influence of crack tip Fracture Process Zone (FPZ). Fakoor (2017) developed a generalized criterion for investigation of fracture in orthotropic materials subjected to mixed mode loading I/II and for any desired crack angle with respect to orthotropic axis. Dissipated energy in fracture process zone has been computed using damage properties while random distribution of micro-cracks are assumed for elastic material. Fakoor and Rafiee (2013) have presented a criterion for predicting crack initiation and propagation in specimens subjected to mixed mode loading I/II. The presented criterion was constructed on the basis of Maximum Shear Stress distribution around the crack tip. Anaraki and Fakoor proposed a mixed mode I/II fracture criterion based on strength properties of composite materials (Anaraki and Fakoor 2011). Some studies have been also conducted for predicting direction of crack propagation in orthotropic materials. Buczek and Herakovich (1985) have presented a criterion in desired planes around crack tip on the basis of tangential stress to tensile strength ratio in anisotroic materials. Gregory and Herkovich (1986) investigated the influence of anisotropic behavior and biaxial loading to identify effective parameters in crack propagation properly. They have employed anisotropic elasticity and FE method and presented three criteria as tangential stress, polynomial tensor and strain energy density for studying crack tip stress field and predicting crack propagation direction. Saouma *et al*. (1987) have presented a MTS-based criterion applicable to orthotropic materials. Critical stress intensity factor along θ -direction was obtained in term of K_{IC}^1 and K_{IC}^2 representing stress intensity factors along elastic axis 1 and 2, respectively. Nobil and Carloni (2005) have analyzed crack in orthotropic plane subjected to biaxial loading. They were intending to investigate the influence of two parameters of orthotropic ratio and biaxial loadings on crack propagation in order to obtain crack propagation direction and geometrical location of fracture. They have employed minimum strain energy density and maximum tangential stress theories and extended them to orthotropic materials. Investigating the effects of biaxial loading on crack propagation, Lim (2012) has used normal stress ratio to predict crack propagation direction.

As it could be found from the above literature, no generalized fracture criterion has been suggested for orthotropic materials subjected to mixed mode loadings I/II in conjunction with real nature of fracture mechanism. Therefore, the main goal of this research is to develop a novel concept for predicting crack propagation in orthotropic materials relying on this fact that fracture of orthotropic materials taken place along fiber and in an isotropic medium. Thus, developed material modeling is called "Equivalent Reinforced Isotropic Material". For this purpose, the well-known Maximum Tangential Stress (MTS) criterion which is basically developed for isotropic materials is extended to orthotropic materials. Experimental observations on orthotropic specimens imply on this fact that a crack always propagate along fibers and in isotropic matrix. Thus, assuming that cracks are placed in isotropic medium and modeling fibers as reinforcements, MTS criterion is extended to orthotropic materials. A good agreement observed between theoretical prediction and experimental observations proved the efficiency of the developed criterion.

2. Extracting mixed mode fracture criterion for an equivalent isotropic material

As shown in Fig. 1 regardless of crack-fiber angle, cracks always propagate in an isotropic medium and along fiber direction in orthotropic materials (Farid and Fakoor, 2019). This inspires that fracture in orthotropic materials follows the fracture mechanism in isotropic materials. So the most important and also comprehensive fracture criterion i.e., Maximum Tangential Stress (MTS) can be extended for investigation of fracture in orthotropic materials.

In orthotropic materials, fibers play the role of reinforcements embedded in an isotropic matrix. Therefore, as it is also evident from Fig. 2, it can be understood that for located cracks along fibers, isotropic matrix experiences fracture phenomena and fibers does not directly affect the

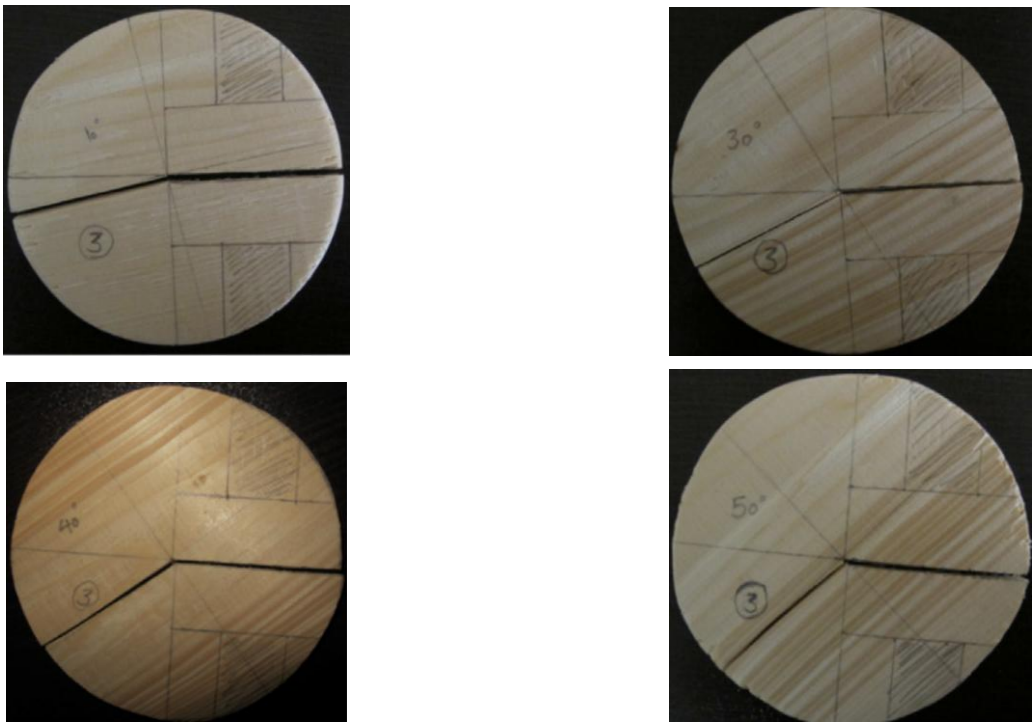

Fig. 1 Propagation of cracks along fiber direction and in isotropic medium between fibers (Farid and Fakoor 2019)

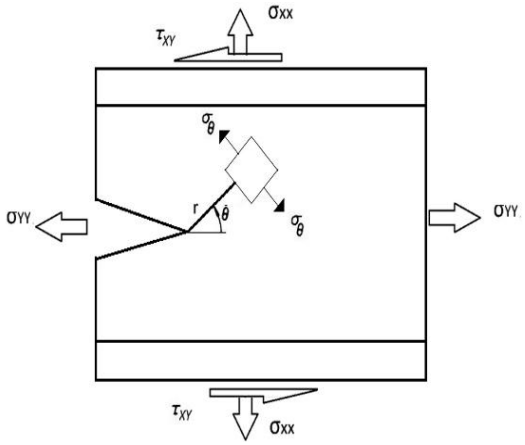

Fig. 2 Crack distribution path and tangential stress around the crack tip of considered RVE in reinforced isotropic material

crack propagation. It is assumed that main role of fiber is to reduce the stress distribution around crack tip and thus MTS will be employed considering this fact.

2.1 Reinforced Isotropic Model (RIM) and Stress Reduction Factors (SRF)

Representative Volume Element (RVE) of a reinforced isotropic material is presented in Fig. 2 Now, Airy stress function can be written for orthotropic material shown in Fig. 2 Far from reinforcement, this stress function will satisfy all equilibrium and compatibility equations. When reinforcements interact with matrix, this strategy is not valid, because equilibrium conditions and strength criterion will not be satisfied for matrix. In this case, Airy stress function has to be written for isotropic matrix material. For a cracked single layer of composite materials in plane-stress conditions, equilibrium equations are written as below in absence of external loadings

$$\frac{\partial \sigma_x}{\sigma_x} + \frac{\partial \tau_{xy}}{\sigma_y} = 0\,, \qquad \frac{\partial \tau_{xy}}{\sigma_x} + \frac{\partial \sigma_y}{\sigma_y} = 0 \tag{1}$$

Constitutive equation is written as below

$$\begin{pmatrix} \varepsilon_x \\ \varepsilon_{yy} \\ \varepsilon_{xy} \end{pmatrix} = \begin{pmatrix} C_{11} & C_{12} & C_{16} \\ C_{21} & C_{22} & C_{26} \\ C_{61} & C_{62} & C_{66} \end{pmatrix} \begin{pmatrix} \sigma_x \\ \sigma_{yy} \\ \sigma_{xy} \end{pmatrix} \tag{2}$$

Due to symmetric configuration of compliance matrix, six independent coefficients are required to be characterized. Compatibility equation is formed as it follows

$$\frac{\partial^2_{\varepsilon_x}}{\partial y^2} + \frac{\partial^2_{\varepsilon_y}}{\partial x^2} = \frac{\partial^2_{\gamma_{xy}}}{\partial x \partial y} \tag{3}$$

For flat crack problems, 2-D solutions can be applied

$$\varepsilon_x = C_{11}\sigma_x + C_{12}\sigma_y\,; \quad \varepsilon_y = C_{12}\sigma_x + C_{22}\sigma_y\,; \quad \gamma_{xy} = C_{66}\tau_{xy} \tag{4}$$

Which can be rearranged in below format

$$\begin{aligned} \varepsilon_x &= \sigma_x/E_x - \nu_{21}\sigma_y/E_y\,; \\ \varepsilon_y &= -\nu_{21}\sigma_x/E_x + \sigma_y/E_y\,; \\ \gamma_{xy} &= \tau_{xy}/G_{xy} \end{aligned} \tag{5}$$

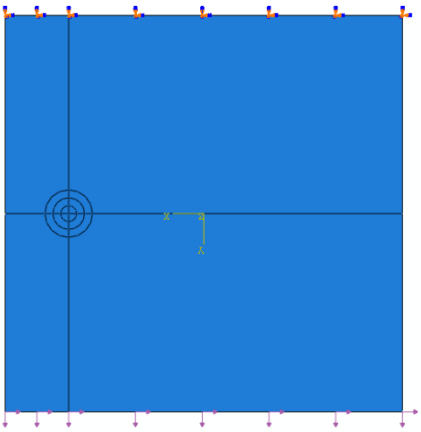

(a) Geometry, loading and boundary conditions

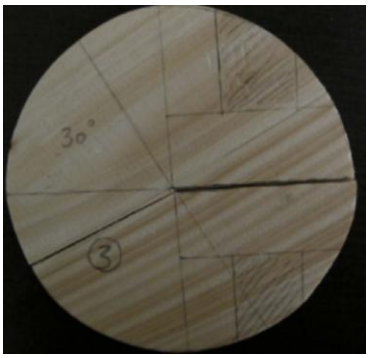

(b) Mesh quality

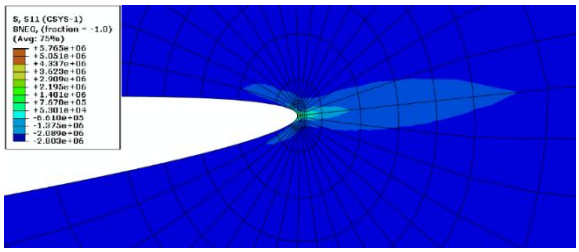

(c) Stress distribution around the crack tip of orthotropic material

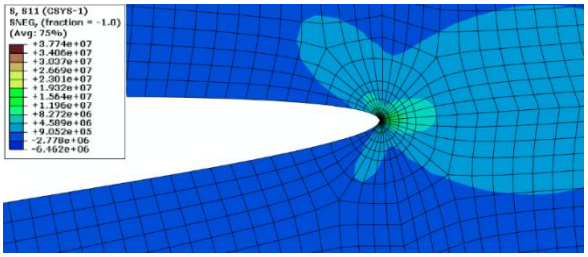

(d) Stress distribution around the crack tip of equivalent isotropic material

Fig. 3 FE model of cracked solids

Therefore, Airy stress function satisfying equilibrium equations is expressed as

$$\sigma_x = \frac{\partial^2 U}{\partial x^2}; \quad \sigma_y = \frac{\partial^2 U}{\partial y^2}; \quad \tau_{xy} = -\frac{\partial^2 U}{\partial x \partial y} \tag{6}$$

Substituting Airy stress functions into Eq. (4) and considering compatibility Eq. (3), we have

$$C_{22}\frac{\partial^4 U}{\partial x^4} + (C_{66} + 2C_{12})\frac{\partial^4 U}{\partial x^2 \partial y^2} + C_{11}\frac{\partial^4 U}{\partial y^4} = 0 \tag{7}$$

Orthotropic materials are reinforced materials wherein fibers are embedded in matrix and initial crack is available in the matrix. Thus, fracture is predicted on the basis of matrix strength and Airy stress function is required to be solved for induced stress components in matrix. Comparing high stiffness of fiber and low stiffness of matrix, there is only one stiffness factor in principal direction which is n times greater. For material with tensile and shear reinforcements, Airy stress function can be modified as below (Van der Put 2007)

$$\frac{\sigma_x}{n_1} = \frac{\partial^2 U}{\partial x^2}; \quad \sigma_y = \frac{\partial^2 U}{\partial y^2}; \quad \frac{\tau_{xy}}{n_6} = -\frac{\partial^2 U}{\partial x \partial y} \tag{8}$$

In which n_1 and n_6 are Stress Reduction Factors (SRF). In fact, reduced stress attributed to the role of reinforcements is analyzed instead of analyzing stress in the crack tip of an orthotropic material. Namely, induced stress components in the matrix of an orthotropic material are a reduced stress with the degree of $n_i (i = 1,6)$ in comparison with overall stress keeping the same compatibility conditions. Substituting these stress functions into compatibility equation, we obtain (Van der Put 2007)

$$C_{22}\frac{\partial^4 U}{\partial x^4} + (n_6 C_{66} + (1 + n_1)C_{12})\frac{\partial^4 U}{\partial x^2 \partial y^2} + n_1 C_{11}\frac{\partial^4 U}{\partial y^4} = 0 \tag{9}$$

n_1 and n_6 should also conforms with below configurations to be able to apply stress function of U to isotropic materials as well

$$n_1 = \frac{C_{22}}{C_{11}} = \frac{E_x}{E_y}; \quad n_6 = \left(2 - \frac{C_{12}}{C_{22}} - \frac{C_{12}}{C_{11}}\right).\frac{C_{22}}{C_{66}} = \left(2 + \nu_{yx} + \nu_{xy}\right)\frac{G_{xy}}{E_y} \tag{10}$$

The hypothesis of Reinforced Isotropic Model (RIM) and definition of Stress Reduction Factors (SRF's) can be verified by Finite Element Method (FEM). Based on aforementioned definition, SRF's could be extracted by comparison of crack tip stress distribution in an orthotropic solid (composition of matrix and fibers) and an isotropic solid which is made of matrix material. Norway spruce wood as a natural orthotropic material has been considered for verification of RIM. FE model of orthotropic material, related isotropic solid and stress distribution around the crack tip are shown in Fig. 3.

Table 1 Elastic (GPa), strength (MPa) and fracture properties ($MPa\sqrt{m}$) of the employed woods

Species	E_y	E_x	G_{xy}	ν_{xy}	T_M	T_m	K_{IC}^{RL}	K_{IIC}^{RL}	K_{IC}^{TL}	K_{IIC}^{TL}
Norway spruce (Picea abies) (Romanowicz and Seweryn 2008)	0.81	11.84	0.63	0.38	63	5.1	0.58	1.52	-	-
Scots pine (Pinus sylvestris) (Jernkvist 2001b)	1.10	16.3	1.74	0.47	52	3.76	0.49	1.32	0.44	2.05
Red spruce (Picea rubens) (Mall *et al*. 1983)	098	12.7	0.80	0.37	84.8	2.4	0.42	1.665	0.42	2.19

Table 2 Results of RIM and FEM

SRF	FEM approach	RIM approach
n_1	$\frac{\sigma_x^{ortho}}{\sigma_x^{iso}} = 13.89$	$\frac{E_x}{E_y} = 14.61$
n_6	$\frac{\sigma_{xy}^{ortho}}{\sigma_{xy}^{iso}} = 1.61$	$(2+\nu_{21}+\nu_{12})\frac{G_{xy}}{E_y} = 1.73$

FE model for Norway spruce wood consist of 10,252 second-order elements and 31,215 nodes is employed to guarantee convergence of the mesh. Crack tip elements are selected as 8-node element and SR8 in order to be able to define quarter point singularity. Also, SR8 second-order element with 8-node is used for other regions. The constructed FE model is presented in Figs. 3(a) and (b). The crack tip region was meshed with the singular quarter point elements with 321 nodes and 92 elements. Crack tip elements are fine enough to satisfy crack tip singularity. Elastic, strength and fracture properties of the utilized materials are in listed in Table 1.

n_1 is defined as the ratio of tensile stress in orthotropic material to isotropic material in x direction (perpendicular to loading direction) and n_6 is the ratio of the shear stress in orthotropic material to isotropic material as follows

$$n_1 = \frac{\sigma_x^{ortho}}{\sigma_x^{iso}}; \quad n_6 = \frac{\sigma_{xy}^{ortho}}{\sigma_{xy}^{iso}} \tag{11}$$

The results of SRF's based on theoretical approach (Eq. 10) and finite element method are compared in Table 2. Therefore, the hypothesis of Reinforced Isotropic Model (RIM) could be acceptable for orthotropic materials.

2.2 Tangential stress at crack tip of reinforced isotropic material

Now, maximum tensile stress around the crack tip is taken into account in accordance with Fig. 2. Erdogan and Sih (1963) have presented MTS as the most important and comprehensive fracture criterion for isotropic materials as follows

$$\sigma_{\theta\theta} = \sigma_{xx}\sin^2(\theta) + \sigma_{yy}\cos^2(\theta) - \tau_{xy}\sin(2\theta) \tag{12}$$

In the above equation, σ_{ij} is the crack tip stress distribution which can be expressed as below

$$\begin{aligned}
\sigma_{xx} &= \frac{K_I}{\sqrt{2\pi r}}\cos\frac{\theta}{2}\left[1-\sin\frac{\theta}{2}\sin\frac{3\theta}{2}\right] \\
&\quad + \frac{K_{II}}{\sqrt{2\pi r}}\sin\frac{\theta}{2}\left[2+\cos\frac{\theta}{2}\cos\frac{3\theta}{2}\right] \\
\sigma_{yy} &= \frac{K_I}{\sqrt{2\pi r}}\cos\frac{\theta}{2}\left[1+\sin\frac{\theta}{2}\sin\frac{3\theta}{2}\right] \\
&\quad + \frac{K_{II}}{\sqrt{2\pi r}}\sin\frac{\theta}{2}\cos\frac{\theta}{2}\cos\frac{3\theta}{2} \\
\tau_{yy} &= \frac{K_I}{\sqrt{2\pi r}}\sin\frac{\theta}{2}\cos\frac{\theta}{2}\cos\frac{3\theta}{2} \\
&\quad + \frac{K_{II}}{\sqrt{2\pi r}}\cos\frac{\theta}{2}\left[1-\sin\frac{\theta}{2}\sin\frac{3\theta}{2}\right]
\end{aligned} \tag{13}$$

Due to aforementioned reasons, it is necessary to consider the effects of fibers as the reinforcements in isotropic matrix for the extension of MTS criterion to orthotropic materials. The effects of fibers can be expressed by n_1, n_6 which are normal and shear stress reduction factors in isotropic matrix, respectively. In other words, new conditions should be considered for matrix reduced stress distribution as below

$$\sigma_{xx} \to \frac{\sigma_x}{n_1}; \quad \tau_{xy} \to \frac{\tau_{xy}}{n_6} \tag{14}$$

Subsequently, sets of Eq. (13) expressing stress distribution at crack tip of an isotropic material are modified or a reinforced isotropic matrix with fibers as below

$$\begin{aligned}
\sigma_{xx} &= \frac{K_I}{n_1\sqrt{2\pi r}}\cos\frac{\theta}{2}\left[1-\sin\frac{\theta}{2}\sin\frac{3\theta}{2}\right] \\
&\quad + \frac{K_{II}}{n_1\sqrt{2\pi r}}\sin\frac{\theta}{2}\left[2+\cos\frac{\theta}{2}\cos\frac{3\theta}{2}\right] \\
\sigma_{yy} &= \frac{K_I}{\sqrt{2\pi r}}\cos\frac{\theta}{2}\left[1+\sin\frac{\theta}{2}\sin\frac{3\theta}{2}\right] \\
&\quad + \frac{K_{II}}{\sqrt{2\pi r}}\sin\frac{\theta}{2}\cos\frac{\theta}{2}\cos\frac{3\theta}{2} \\
\tau_{yy} &= \frac{K_I}{n_6\sqrt{2\pi r}}\sin\frac{\theta}{2}\cos\frac{\theta}{2}\cos\frac{3\theta}{2} \\
&\quad + \frac{K_{II}}{n_6\sqrt{2\pi r}}\cos\frac{\theta}{2}\left[1-\sin\frac{\theta}{2}\sin\frac{3\theta}{2}\right]
\end{aligned} \tag{15}$$

Substituting Eq. (15) into Eq. (12), extended maximum tangential stress is obtained for an equivalent reinforced isotropic material with fiber as follows

$$\sigma_{\theta\theta} = \frac{K_I}{n_1 n_6\sqrt{2\pi r}}\Big[\frac{n_6}{4}\Big(2\cos\frac{\theta}{2}-\cos\frac{3\theta}{2}-\cos\frac{5\theta}{2}\Big) -\frac{n_6}{16}\Big(3\cos\frac{\theta}{2}-\cos\frac{3\theta}{2}-3\cos\frac{5\theta}{2}+\cos\frac{9\theta}{2}\Big) +\frac{n_1 n_6}{4}\Big(2\cos\frac{\theta}{2}+\cos\frac{3\theta}{2}+\cos\frac{5\theta}{2}\Big) +\frac{n_1 n_6}{16}\Big(\cos\frac{\theta}{2}-\cos\frac{3\theta}{2}-\cos\frac{5\theta}{2}-\cos\frac{9\theta}{2}\Big) -\frac{n_1}{8}\Big(\cos\frac{\theta}{2}-\cos\frac{3\theta}{2}+\cos\frac{5\theta}{2}-\cos\frac{9\theta}{2}\Big)\Big] +\frac{K_{II}}{n_1 n_6\sqrt{2\pi r}}\Big[-\frac{n_6}{2}\Big(2\sin\frac{\theta}{2}-\sin\frac{3\theta}{2}-\sin\frac{5\theta}{2}\Big) +\frac{n_6}{16}\Big(3\sin\frac{\theta}{2}-\sin\frac{3\theta}{2}-3\sin\frac{5\theta}{2}+\sin\frac{9\theta}{2}\Big) +\frac{n_1 n_6}{4}\Big(-\sin\frac{\theta}{2}+\sin\frac{3\theta}{2}+\sin\frac{5\theta}{2}+\sin\frac{9\theta}{2}\Big) +\frac{n_1}{8}\Big(\sin\frac{\theta}{2}+\sin\frac{3\theta}{2}+\sin\frac{5\theta}{2}-\sin\frac{9\theta}{2}\Big) -\frac{n_1}{2}\Big(\sin\frac{3\theta}{2}+\sin\frac{5\theta}{2}\Big)\Big] \quad (16)$$

2.3 Predicting crack propagation direction

It is assumed that crack propagates in an isotropic medium when tangential stress at angle $\boldsymbol{\theta_0}$ reaches its critical value of $\sigma_{\theta\theta}$. Thus, fracture occurs in isotropic field when below conditions are satisfied

$$\begin{cases} \theta = \theta_0 \\ \sigma_{\theta\theta} = \sigma_{\theta\theta c} \end{cases} \quad (17)$$

For pure mode I loading (i.e., $K_{II} = 0$) we have

$$\sigma_{\theta\theta c} = \frac{K_{Ic}}{\sqrt{2\pi r}} \quad (18)$$

Thus, substituting Eq. (18) into Eq. (16), a relationship between stress intensity factors and critical stress intensity factor is established as below

$$\frac{K_I}{n_1 n_6 K_{Ic}\sqrt{2\pi r}}\Big[\frac{n_6}{4}\Big(2\cos\frac{\theta}{2}-\cos\frac{3\theta}{2}-\cos\frac{5\theta}{2}\Big) -\frac{n_6}{16}\Big(3\cos\frac{\theta}{2}-\cos\frac{3\theta}{2}-3\cos\frac{5\theta}{2}+\cos\frac{9\theta}{2}\Big) +\frac{n_1 n_6}{4}\Big(2\cos\frac{\theta}{2}+\cos\frac{3\theta}{2}+\cos\frac{5\theta}{2}\Big) +\frac{n_1 n_6}{16}\Big(\cos\frac{\theta}{2}-\cos\frac{3\theta}{2}-\cos\frac{5\theta}{2}-\cos\frac{9\theta}{2}\Big) -\frac{n_1}{8}\Big(\cos\frac{\theta}{2}-\cos\frac{3\theta}{2}+\cos\frac{5\theta}{2}-\cos\frac{9\theta}{2}\Big)\Big] +\frac{K_{II}}{n_1 n_6 K_{IIc}\sqrt{2\pi r}} \Big[-\frac{n_6}{2}\Big(2\sin\frac{\theta}{2}-\sin\frac{3\theta}{2}-\sin\frac{5\theta}{2}\Big) +\frac{n_6}{16}\Big(3\sin\frac{\theta}{2}-\sin\frac{3\theta}{2}-3\sin\frac{5\theta}{2}+\sin\frac{9\theta}{2}\Big) \quad (19)$$

Table 3 Theoretical proposed mixed mode fracture criteria for orthotropic materials

Author	Based on	Criterion formulation
Jernkvist (2001a, b)	Minimum strain energy release rate	$K_I^2 + \beta_1 K_{II}^2 = K_{IC}^2, \quad \beta_1 = \left(\frac{K_{IC}}{K_{IIC}}\right)^2$
Jernkvist (2001a, b)	Maximum strain energy density	$K_I^2 + {}^1/_{\beta_1} K_{II}^2 = K_{IC}^2, \quad {}^1/_{\beta_1} = \left(\frac{K_{IC}}{K_{IIC}}\right)^2$
Jernkvist (2001a, b)	Maximum principal stress	$\frac{1}{\beta_3+\sqrt{\beta_4}}\left[\beta_3 K_I + \sqrt{\beta_4 K_I^2 + K_{II}^2}\right] = K_{Ic}$ $\beta_3 + \sqrt{\beta_4} = \frac{K_{IIC}}{K_{IC}}$
Romanowicz and Seweryn (2008)	Nonlocal stress	$K_I^2 + \rho_c K_{II}^2 = K_{IC}^2, \quad \rho_c = \frac{C_{RL}}{C_R} = \left(\frac{K_{IC}}{K_{IIC}}\right)^2$
Anaraki and Fakoor (2010b)	Reinforced micro crack model	$K_I^2 + \rho_c K_{II}^2 = K_{Ic}$ $\rho_c = \frac{(5-\nu)(\xi\sqrt{\lambda}+\nu_{LR}\lambda)^2}{(10-3\nu)(1+0.5\nu_{LR}(1+\lambda))^2}$
Anaraki and Fakoor (2010a)	Maximum strain energy released rate	$K_I^2 + \rho K_{II}^2 - K_{Ic} = 0, \rho = (\sqrt{C_{11}^{'}/C_{22}^{'}})_{damage}$
Fakoor and Rafiee (2013)	Maximum shear stress	$K_I^2 + \rho K_{II}^2 - K_{Ic} = 0 \quad , \rho = \left(\frac{K_{IC}}{K_{IIC}}\right)^2$
Anaraki and Fakoor (2011)	Strength based criterion	$K_I^2 + \rho_c K_{II}^2 - K_{Ic} = 0\,, \quad \rho_c = 2\left[\frac{T_m}{T_M} + \left(\frac{T_m}{T_M}\right)^2\right]$

Table 4 Empirical fracture criteria for orthotropic material

Investigator	Criterion formulation
Tsai and Wu (1971)	$\left(\frac{K_I}{K_{IC}}\right)+(\frac{K_{IC}}{K_{IIC}})^2=1$
Sih *et al*. (1975)	$S=\beta_{11}K_I^2+\beta_{12}K_IK_{II}+\beta_{22}K_{II}^2$
Williams and Birch (1976)	$\frac{K_I}{K_{IC}}=1$
Leicester (1974)	$K_I+(\frac{K_{IC}}{K_{IIC}})K_{II}-K_{IC}=0$
Hunt and Croager (1982)	$K_I+\left[(1.005)\frac{K_{IC}}{K_{IIC}^{3.4}}\right]K_{II}^{3.4}-1=0$
Mall *et al*. (1982)	$K_I+\left[\frac{K_{IC}}{K_{IIC}^2}\right]K_{II}^2-1=0$

$$+\frac{n_1n_6}{4}\left(-\sin\frac{\theta}{2}+\sin\frac{3\theta}{2}+\sin\frac{5\theta}{2}+\sin\frac{9\theta}{2}\right)$$
$$+\frac{n_1}{8}\left(\sin\frac{\theta}{2}+\sin\frac{3\theta}{2}+\sin\frac{5\theta}{2}-\sin\frac{9\theta}{2}\right) \quad (19)$$
$$-\frac{n_1}{2}\left(\sin\frac{3\theta}{2}+\sin\frac{5\theta}{2}\right)\Big]=1$$

Above equation could be considered as Extended Maximum Tensile Stress (EMTS) criterion which is obtained by extending MTS to orthotropic materials wherein orthotropic material is treated as an Equivalent Reinforced Isotropic Material (ERIM). Following we will confirm that the results of the proposed criterion are in accordance with the nature of fracture of orthotropic materials.

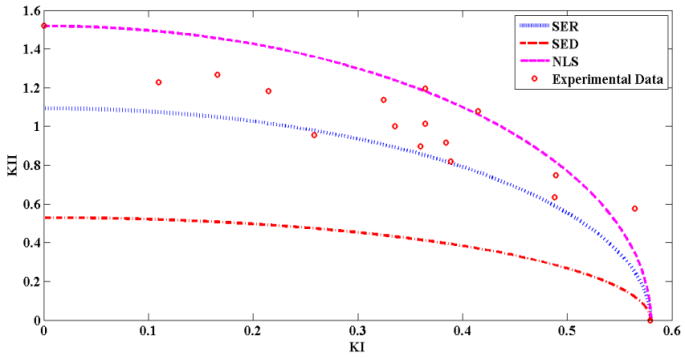

(a) Norway spruce wood (Jernkvist 2001b)

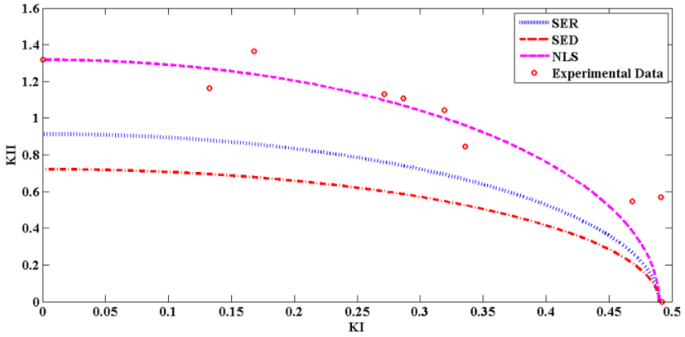

(b) Scot Pine wood (Romanowicz and Seweryn 2008)

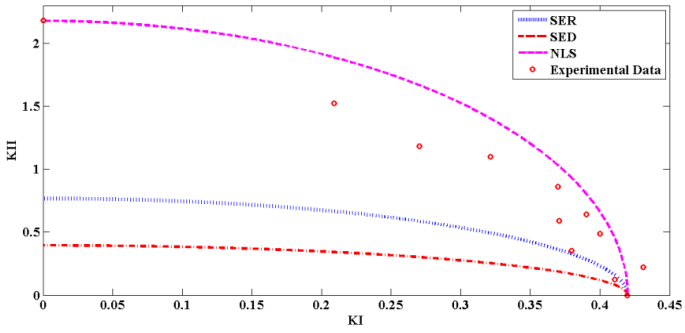

(c) Red Spruce wood (Jernkvist 2001b)

Fig. 4 Fracture limit curves for mixed mode loading in comparison with experimental data ($K_I, K_{II}(Mpa\sqrt{m})$

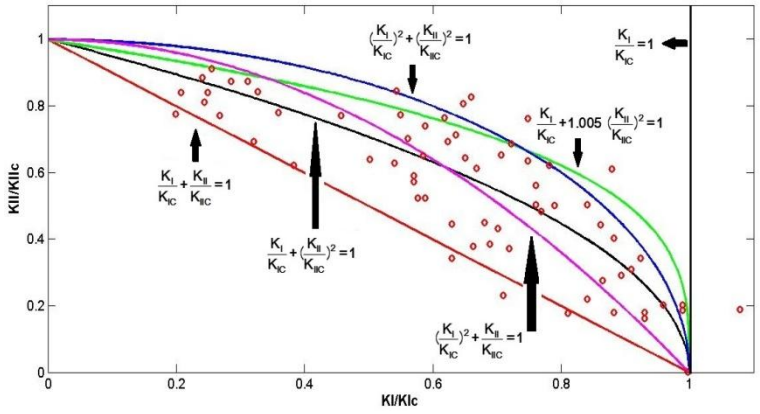

Fig. 5 Comparing empirical fracture limits curves for mixed mode loading

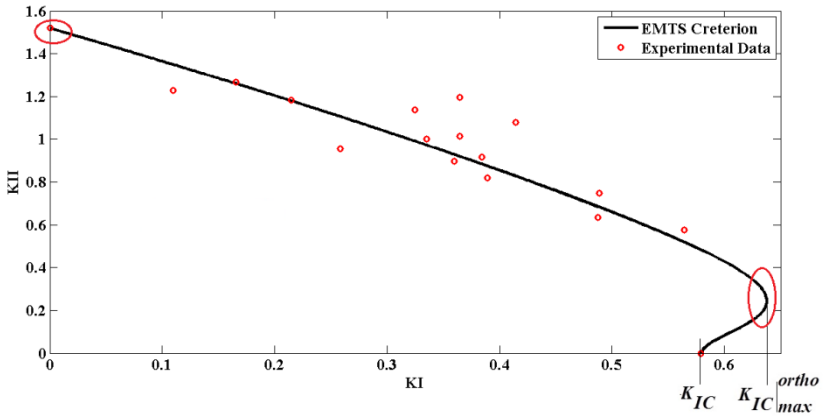

Fig. 6 Fracture limit curve utilizing EMTS in comparison with experimental data ($K_I, K_{II}(Mpa\sqrt{m})$ (Jernkvist 2001b) and Concept of maximum orthotropic fracture toughness in mode I ($K_{Ic}|^{ortho}_{max}$)

3. Investigation of available mixed-mode fracture criteria for orthotropic materials

In this section a review has been performed on available mixed mode I/II fracture criteria to introduce the drawbacks and limitations. These presented criteria can be divided it to two general kinds; named here as theoretical and empirical. General forms of presented theoretical mixed-mode fracture criteria for orthotropic materials are collected from literature and presented in Table 3. Also there are some empirical fracture criteria which are based on cure fitting on experimental data for orthotropic materials that summarized in Table 4.

Fracture limit curves for different types of composite materials consisting Norway spruce, Scots Pine and Red spruce woods are presented in Fig. 4 and compared with experimental data. It can be interpreted from Fig. 4 that energy-based criteria (i.e., extended SER and SED) are too conservative, especially for mode II-dominated loading conditions. Also employing Non-local stress criterion needs pure mode II fracture toughness data which is not available in the literature due to test difficulties.

Fig. 5 presents fracture limit curves for empirical criteria (see Table 4) in comparison with experimental fracture data for Balsa wood (Wu 1967).

4. Investigation of results of extended maximum tensile stress criterion

In Fig. 6, fracture limit curve obtained through EMTS criterion for Norway spruce wood is presented. As it can be seen from Fig. 6 developed EMTS criterion predicts results in a good agreement with experimental data. The compatibility of trend of proposed fracture limit curve with real fracture mechanism is discussed in this section.

In contrast to available fracture criteria for orthotropic material under mixed mode loadings, as it is evident from Fig. 6 that fracture limit curve exceeds K_{Ic} at a specific point highlighted by $K_{Ic}|^{ortho}_{max}$. This means that the investigated specimen can tolerate more loading than critical load associated with pure mode I loading. In fact, load bearing capacity of orthotropic materials subjected to mixed mode loading I/II is higher than that of pure mode I loading. This fact has not been reported by other available mixed mode fracture criteria. Also another fact which confirms the superiority of the EMTS criterion is also shown in Fig. 6. Good agreement between experimental data and theoretically estimation for pure mode II fracture toughness (K_{IIc}) is evident in this Fig. This coincidence has not been reported by other available criteria. Fig. 6

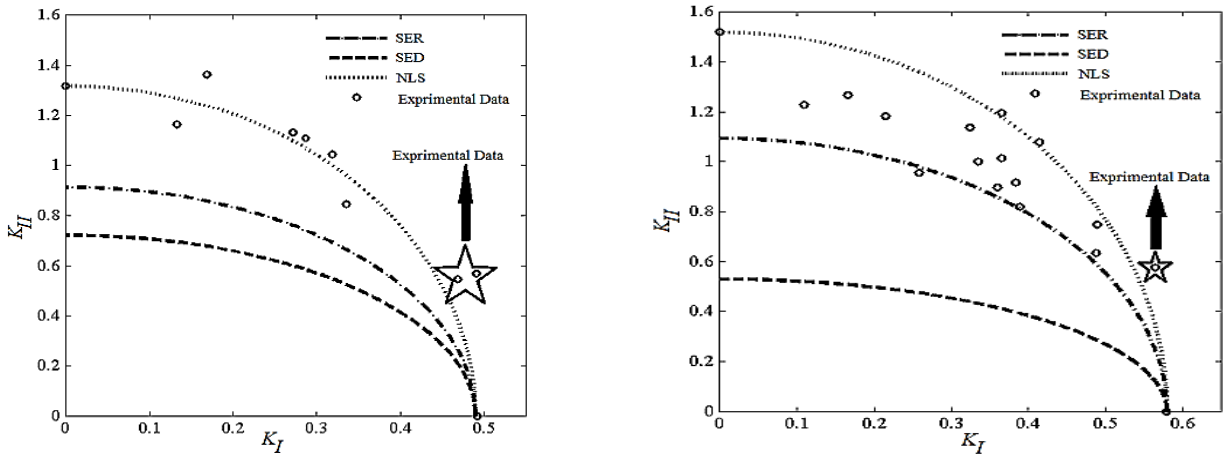

(a) Scots pine wood (b) Norway spruce wood

Fig. 7 Experimental data exceed from available fracture limit curves ($K_I, K_{II}(Mpa\sqrt{m})$ (Jernkvist 2001b)

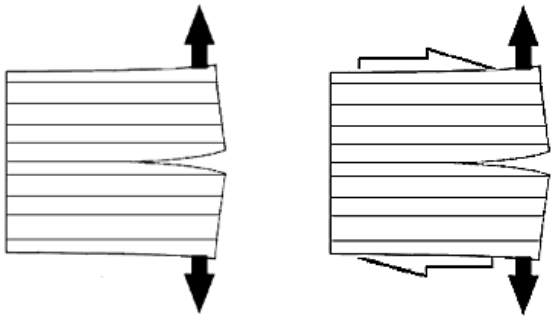

(a) Pure mode I loading (b) Mixed mode loading

Fig. 8 Orthotropic plate under

presented the results of EMTS for Norway spruce wood with introduced material properties in Table 1. As it is shown in Fig. 6, developed EMTS is not only able to predict aforementioned toughening behavior but also it can estimated K_{IIc}.

5. New fracture mechanics property for orthotropic materials ($K_{Ic}|^{ortho}_{max}$)

Experimental observations reported in published data (Hunt and Croager 1982, Jernkvist 2001a, b) for orthotropic materials under mixed mode I/II loadings, show that some experimental data cannot be captured at all by any proposed fracture criteria as it has been presented in Fig 7. This specific region has been perfectly addressed by developed EMTS criterion. This region implies on this fact that a cracked orthotropic material shows more strength in mixed mode loading in comparison with pure mode I. A new material property named here as maximum orthotropic fracture toughness in mode I ($K_{Ic}|^{ortho}_{max}$) can be defined for orthotropic materials accordingly. As it could be found from Fig. 7, for highlighted experimental data $K_{Ic} > K_{Ic}$.

This toughening mechanism can be interpreted from physical point of view as shown in Fig. 8. In orthotropic materials with cracks along fiber, crack propagation occurs in isotropic matrix. According to Fig. 8 (a), in pure mode I the load vector is perpendicular to fibers and therefore fibers do not contribute in preventing crack propagation at this specific case. But, when shear loading is also applied in to the specimen (see Fig. 8 (b)), mixed mode loading is pertinent to investigated case. In this case, fibers will be activated and contribute in load bearing so the applied stress at crack tip will be reduces and prevent crack propagation practically. Developed EMTS criterion takes into account this phenomenon using n_1, n_6 coefficients. In other words, the investigated specimen can accommodate more loadings in comparison with pure mode I loading and thus skewness to the right hand is observed in both experimental data and theoretical fracture limit curve estimated by ESTM model.

As a matter of fact, $K_{Ic}|^{ortho}_{max}$ represents maximum load bearing capacity of orthotropic materials that can be captured in mode I axis (see Fig. 6) and can be introduces as a new developed material property. A portion of loading in mode I and II which presents $K_{Ic}|^{ortho}_{max}$ can be considered as an angle between fiber and crack direction. This concept is schematically shown in Fig. 9. As it is depicted in Fig. 9, ω angle can be defined in a manner that contribution of shear loading τ and tensile loading σ result in $K_{Ic}|^{ortho}_{max}$ The ω is hereafter referred as

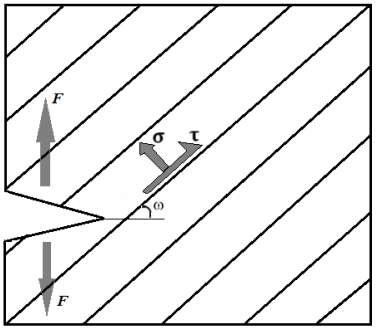

Fig. 9 Force Components on crack edges

optimum angle between fiber and crack. This specific angle represents maximum load bearing capacity in notched orthotropic materials.

6. Optimum angle between fiber and crack for maximum load bearing capacity

In order to extend the concept of optimum angle between fiber and crack for the purpose of maximizing load bearing capacity, converting tensile-shear loading to pure normal loading conditions with suitable fiber orientation is needed. This concept is shown in Fig. 10. For determination of equivalent fiber-crack angle in which tensile-shear loading of point *A* in Fig. 11 could be reflected, contribution of both tensile and shear loadings needs to be computed.

Stress intensity factors are calculated employing analytical formulations. The relation between stress concentration factors and the angle between fiber and crack are mentioned in different references as below equations (Jernkvist 2001a)

$$\begin{cases} K_I = \sigma\sqrt{\pi a} f_I(\varphi) \\ K_{II} = \sigma\sqrt{\pi a} f_{II}(\varphi) \end{cases} \tag{20}$$

where

$$\begin{cases} f_I(\varphi) = 3.028 - 3.22 \times 10^{-3}\varphi \\ +3.73 \times 10^{-4}\varphi^2 - 9.14 \times 10^{-6}\varphi^3 \\ f_I(\varphi) = \sin(2\varphi)\,(0.644 + 4.89 \times 10^{-3}\varphi) \end{cases} \tag{21}$$

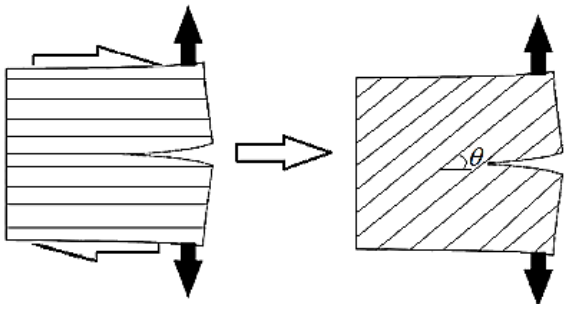

Fig. 10 Conversion of tensile-shear loading to pure tensile loading with fiber orientation

Recalling from Fig. 11, $\theta_{,opt}$ can be calculated using above equations when stress intensity factors are obtained

$$K_{I,opt} = 0.63799\,, \quad K_{II,opt} = 0.241935 \tag{22}$$

Finally, for Norway Spruce we have this

$$\theta_{,opt} = 53.28^{\circ} \tag{23}$$

Similarity for other woods we obtain

$$\begin{cases} Scots\ Pine \rightarrow \theta_{,opt} = 53.29^{\circ} \\ Red\ Spruse \rightarrow \theta_{,opt} = 45.43^{\circ} \end{cases} \tag{24}$$

The results demonstrate that optimum angle between crack and fiber direction is about 50°. In other words, if it is intended to create a notch in an orthotropic specimen, it should be located at $\theta_{,opt}$ direction with respect to fiber direction. This optimum angle was obtained between $40^{\circ} - 50^{\circ}$ in Fakoor *et al.* (2015). Moreover, this optimum angle implies on more resistance against crack propagation.

7. Conclusions

In this research, a novel mixed mode I/II fracture criterion named as Extended Maximum Tensile Stress (EMTS) is presented for orthotropic materials. This criterion is developed based on extension of MTS which is widely used for isotropic materials. A new concept of Equivalent Reinforced Isotropic Material (ERIM) is developed to extend available MTS criterion in to orthotropic materials. ERIM model is based on several experimental observations in which regardless of crack inclination with respect to fibers, cracks always propagate in isotropic medium and along the fiber direction. In this model, stress components are reduced by defined stress reduction factors. The proposed material model was approved by finite element analysis. According to obtained fracture limit curves, a new material property was defined for cracked orthotropic specimens which called here as mode I maximum orthotropic fracture toughness. A comparison between experimental data and theoretical estimation proves the proficiency of developed criterion for predicting fracture behavior of orthotropic materials.

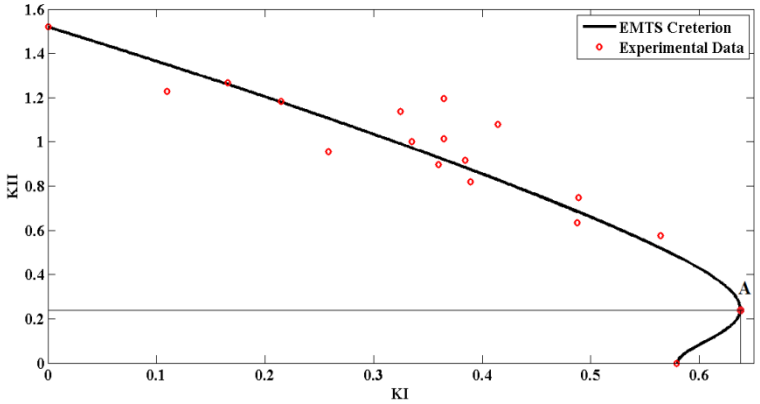

Fig. 11 Determining tensile and shear loading contributions at maximum load bearing capacity ($K_I, K_{II}(Mpa\sqrt{m})$

References

Al-Fasih, M.Y., Kueh, A.B.H., Sabah, S.H. and Yahya, M.Y. (2018), "Tow waviness and anisotropy effects on Mode II fracture of triaxially woven composite", *Steel Compos. Struct., Int. J.*, **26**(2), 241-253.

Aliha, M.R.M., Bahmani, A. and Akhondi, S. (2015), "Determination of mode III fracture toughness for different materials using a new designed test configuration", *Mater. Des.*, **86**, 863-871.

Anaraki, A.G. and Fakoor, M. (2010a), "General mixed mode I/II fracture criterion for wood considering T-stress effects", *Mater. Des.*, **31**(9), 4461-4469.

Anaraki, A.G. and Fakoor, M. (2010b), "Mixed mode fracture criterion for wood based on a reinforcement micro-crack damage model", *Mater. Sci. Eng.: A*, **527**(27), 7184-7191.

Anaraki, A.G. and Fakoor, M. (2011), "A new mixed-mode fracture criterion for orthotropic materials, based on strength properties", *J. Strain Anal. Eng. Des.*, **46**(1), 33-44.

Buczek, M.B. and Herakovich, C.T. (1985), "A normal stress criterion for crack extension direction in orthotropic composite materials", *J. Compos. Mater.*, **19**(6), 544-553.

Cetisli, F. and Kaman, M.O. (2014), "Numerical analysis of interface crack problem in composite plates jointed with composite patch", *Steel Compos. Struct., Int. J.*, **16**(2), 203-220.

Chow, C.L. and Woo, C.W. (1979), "Orthotropic and mixed mode fracture in wood", *Proceedings of the 1st International Conference of Wood Fracture*, Vancouver, Canada, pp. 39-52.

Deretic-Stojanovic, B. and Kostic, S.M. (2017), "A simplified matrix stiffness method for analysis of composite and prestressed beams", *Steel Compos. Struct., Int. J.*, **24**(1), 53-63.

Ehart, R.J.A., Stanzl-Tschegg, S.E. and Tschegg, E.K. (1998), "Crack face interaction and mixed mode fracture of wood composites during mode III loading", *Eng. Fract. Mech.*, **61**(2), 253-278.

Erdogan, F. and Sih, G.C. (1963), "On the crack extension in plates under plane loading and transverse shear", *J. Basic Eng.*, **85**(4), 519-525.

Faal, R.T., Aghsam, A. and Milani, A.S. (2015), "Stress intensity factors for cracks in functionally graded annular planes under anti-plane loading", *Int. J. Mech. Sci.*, **93**, 73-81.

Fakoor, M. (2017), "Augmented Strain Energy Release Rate (ASER): A novel approach for investigation of mixed-mode I/II fracture of composite materials", *Eng. Fract. Mech.*, **179**, 177-189.

Fakoor, M. and Khansari, N.M. (2016), "Mixed mode I/II fracture criterion for orthotropic materials based on damage zone properties", *Eng. Fract. Mech.*, **153**, 407-420.

Fakoor, M. and Rafiee, R. (2013), "Fracture investigation of wood under mixed mode I/II loading based on the maximum shear stress criterion", *Strength Mater.*, **45**(3), 378-385.

Fakoor, M., Rafiee, R. and Sheikhansari, M. (2015), "The influence of fiber-crack angle on the crack tip parameters in orthotropic materials", *Proceedings of the Institution of Mechanical Engineers, Part C: Journal of Mechanical Engineering Science*, **231**(3), 418-431.

Farid, H.M. and Fakoor, M. (2019), "Mixed Mode I/II Fracture Criterion for Arbitrary Cracks in Orthotropic Materials Considering T-Stress Effects", *Theor. Appl. Fract. Mech.*, **99**, 147-160.

Golewski, G.L. (2017a), "Effect of fly ash addition on the fracture toughness of plain concrete at third model of fracture", *J. Civil Eng. Manag.*, **23**(5), 613-620.

Golewski, G.L. (2017b), "Generalized fracture toughness and compressive strength of sustainable concrete including low calcium fly ash", *Materials*, **10**(12), 1393.

Golewski, G.L. (2017c), "Determination of fracture toughness in concretes containing siliceous fly ash during mode III loading", *Struct. Eng. Mech., Int. J.*, **62**(1), 1-9.

Gregory, M.A. and Herakovich, C.T. (1986), "Predicting crack growth direction in unidirectional composites", *J. Compos. Mater.*, **20**(1), 67-85.

Hunt, D.G. and Croager, W.P. (1982), "Mode II fracture toughness of wood measured by a mixed-mode test method", *J. Mater. Sci. Lett.*, **1**(2), 77-79.

Jernkvist, L.O. (2001a), "Fracture of wood under mixed mode loading: I. Derivation of fracture criteria", *Eng. Fract. Mech.*, **68**(5), 549-563.

Jernkvist, L.O. (2001b), "Fracture of wood under mixed mode loading: II. Experimental investigation of Picea abies", *Eng. Fract. Mech.*, **68**(5), 565-576.

Lazzarin, P., Campagnolo, A. and Berto, F. (2014), "A comparison among some recent energy-and stress-based criteria for the fracture assessment of sharp V-notched components under Mode I loading", *Theor. Appl. Fract. Mech.*, **71**, 21-30.

Leicester, R.H. (1974), "Application of Linear Fracture Mechanics in the Design of Timber Structures", *Proceedings, Conference Australian Fractured Group 23*, Melbourne, Australia, October, pp. 156-164.

Li, J., Meng, S., Tian, X., Song, F. and Jiang, C. (2012), "A non-local fracture model for composite laminates and numerical simulations by using the FFT method", *Compos. Part B: Eng.*, **43**(3), 961-971.

Lim, W.K. (2012), "Mixed-mode crack extension in orthotropic materials under biaxial load", *Int. J. Fract.*, **173**(1), 71-77.

Mall, S., Murphy, J.F. and Shottafer, J.E. (1983), "Criterion for mixed mode fracture in wood", *J. Eng. Mech.*, **109**(3), 680-690.

Merzoug, M., Boulenouar, A. and Benguediab, M. (2017), "Numerical analysis of the behaviour of repaired surface cracks with bonded composite patch", *Steel Compos. Struct., Int. J.*, **25**(2), 209-216.

Motamedi, D. and Mohammadi, S. (2012), "Fracture analysis of composites by time independent moving-crack orthotropic XFEM", *Int. J. Mech. Sci.*, **54**(1), 20-37.

Nobile, L. and Carloni, C. (2005), "Fracture analysis for orthotropic cracked plates", *Compos. Struct.*, **68**(3), 285-293.

Romanowicz, M. and Seweryn, A. (2008), "Verification of a non-local stress criterion for mixed mode fracture in wood", *Eng. Fract. Mech.*, **75**(10), 3141-3160.

Sadowski, T. and Golewski, G.L. (2018), "A failure analysis of concrete composites incorporating fly ash during torsional loading", *Compos. Struct.*, **183**, 527-535.

Saouma, V.E., Ayari, M.L. and Leavell, D.A. (1987), "Mixed mode crack propagation in homogeneous anisotropic solids", *Eng. Fract. Mech.*, **27**(2), 171-184.

Serier, N., Mechab, B., Mhamdia, R. and Serier, B. (2016), "A new formulation of the J integral of bonded composite repair in aircraft structures", *Struct. Eng. Mech., Int. J.*, **58**(5), 745-755.

Sih, G.C., Paris, P.C. and Irwin, G.R. (1965), "On cracks in rectilinearly anisotropic bodies", *Int. J. Fract. Mech.*, **1**(3), 189-203.

Sih, G.C., Chen, E.P., Huang, S.L. and McQuillen, E.J. (1975), "Material characterization on the fracture of filament-reinforced composites", *J. Compos. Mater.*, **9**(2), 167-186.

Tsai, S.W. and Wu, E.M. (1971), "A general theory of strength for anisotropic materials", *J. Compos. Mater.*, **5**(1), 58-80.

Van der Put, T.A.C.M. (2007), "A new fracture mechanics theory for orthotropic materials like wood", *Eng. Fract. Mech.*, **74**(5), 771-781.

Williams, J.G. and Birch, M.W. (1976), "Mixed mode fracture in anisotripic media", *ASTM STP*, p. 125-137.

Wu, E.M. (1967), "Application of fracture mechanics to anisotropic plates", *J. Appl. Mech.*, **34**(4), 967-974.

Nomeclature

a	Crack length
C_{ij}	Components of compliance matrix
E	Young's moduli of the matrix
$E_i = x, y, z$	Young's moduli in the *i* direction
G	Strain energy release rate
$G_{ij} = x, y, z$	Shear modulus
K_I, K_{II}	Modes *I* and *II* stress intensity factor
K_{IC}, K_{IIC}	Modes *I* and *II* fracture toughness
L, R, T	Axes of orthotropy in wood
T_M	Tensile strength of the orthotropic material in fiber direction
T_m	Tensile strength of the orthotropic material perpendicular to fiber direction
$n_i, i = 1, 6$	Normal and shear reinforcement effects
U	Airy stress functions
$\varepsilon_{ij}, \gamma_{ij}$	The normal and shear Strains
ν_{ij}	Poisson's ratio
ρ	Orthotropic damage factor
σ_{ij}, τ_{ij}	The normal and shear stress around the crack tip
$\sigma_{\theta\theta}$	Maximum tangential stress
θ_0	Crack growth angle
ω	Crack-fiber angle